J. Cell. Mol. Med. Vol 14, No 6B, 2010 pp. 1408-1418

Imatinib inhibits vascular smooth muscle proteoglycan synthesis and reduces LDL binding *in vitro* and aortic lipid deposition *in vivo*

Mandy L. Ballinger [a], Narin Osman [a, b], Kazuhiko Hashimura [c], Judy B. de Haan [d], Karin Jandeleit-Dahm [d], Terri Allen [d], Lisa R. Tannock [e], John C. Rutledge [f], Peter J. Little [a, b, g, *]

[a] *Diabetes & Cell Biology, BakerIDI Heart & Diabetes Institute, Prahran, Australia*
[b] *Department of Immunology, Monash University, Melbourne, Australia*
[c] *National Cardiovascular Centre, Osaka, Japan*
[d] *Diabetic Complications Research Group, Baker IDI Heart & Diabetes Institute, Prahran, Australia*
[e] *Division of Endocrinology and Molecular Medicine, University of Kentucky, Lexington, KY, USA*
[f] *Division of Endocrinology, Clinical Nutrition and Vascular Medicine, University of California, CA, USA*
[g] *Department of Medicine, Monash University, Melbourne, Australia*

Received: June 14, 2009; Accepted: August 17, 2009

Abstract

The 'response to retention' hypothesis of atherogenesis proposes that proteoglycans bind and retain low-density lipoproteins (LDL) in the vessel wall. Platelet-derived growth factor (PDGF) is strongly implicated in atherosclerosis and stimulates proteoglycan synthesis. Here we investigated the action of the PDGF receptor inhibitor imatinib on PDGF-mediated proteoglycan biosynthesis *in vitro*, lipid deposition in the aortic wall *in vivo* and the carotid artery *ex vivo*. In human vSMCs, imatinib inhibited PDGF mediated ^{35}S-SO_4 incorporation into proteoglycans by 31% ($P < 0.01$) and inhibited PDGF-mediated size increases in both chemically cleaved and xyloside associated glycosaminoglycan (GAG) chains by 19%, $P < 0.05$ and 27%, $P < 0.05$, respectively. Imatinib decreased PDGF stimulation of the 6:4 position sulphation ratio of disaccharides. The half maximal saturation value for LDL binding for proteoglycans from PDGF stimulated cells in the presence of imatinib was approximately 2.5-fold higher than for PDGF treatment alone. In high fat fed ApoE$^{-/-}$ mice, imatinib reduced total lipid staining area by ~31% ($P < 0.05$). Carotid artery lipid accumulation in imatinib treated mice was also reduced. Furthermore, we demonstrate that imatinib inhibits phosphorylation of tyrosine 857, the autophosphorylation site of the PDGF receptor, in vSMCs. Thus imatinib inhibits GAG synthesis on vascular proteoglycans and reduces LDL binding *in vitro* and *in vivo* and this effect is mediated *via* the PDGF receptor. These findings validate a novel mechanism to prevent cardiac disease.

Keywords: atherosclerosis • proteoglycans • vascular smooth muscle • glycosaminoglycans • protein tyrosine kinase

Introduction

Cardiovascular disease is the major cause of premature mortality in Western societies [1]. The major underlying process is atherosclerosis leading to the formation of unstable plaques followed by thrombotic occlusion of the coronary arteries, myocardial ischemia, heart failure and death [2]. Recently it has been definitively demonstrated that in human atherosclerosis the pathological process commences with the deposition of lipid in areas of diffuse intimal thickenings [3, 4]. The deposition of lipid in early human lesions occurs in association with enrichment in the proteoglycan, biglycan [3]. This finding strongly supports the 'response to retention' hypothesis of atherogenesis, which states that the sub-endothelial binding and retention of atherogenic lipoproteins by matrix molecules is a critical step [5]. Ionic interactions form the basis for retention of atherogenic lipoproteins. Positively charged residues on the apolipoprotein of low-density

*Correspondence to: Prof. Peter J. LITTLE,
Head, Diabetes & Cell Biology, Baker IDI Heart & Diabetes Institute,
St. Kilda Road Central PO Box 6492, Melbourne 8008 Victoria, Australia.
Tel.: +61 3 8532 1203
Fax: +61 3 8532 1100
E-mail: peter.little@bakeridi.edu.au

doi:10.1111/j.1582-4934.2009.00902.x

lipoprotein (LDL) bind to negatively charged glycosaminoglycan (GAG) chains on proteoglycans. It has been speculated that growth factor-induced changes in the GAG chains bestow a greater attraction for lipid and is a crucial step for the atherosclerotic cascade that follows [3, 6–8].

Platelet-derived growth factor (PDGF) stimulates the production and increases the size of proteoglycans, with the latter response due to elongation of GAG chains [9, 10]. PDGF stimulates the expression of mRNA for proteoglycan core proteins, specifically, versican [10] and PDGF also increases the 6:4 position sulphation ratio of disaccharides [9]. Imatinib, is a small molecule tyrosine kinase inhibitor used for the treatment of human chronic myeloid leukaemia [11]. Imatinib is a 2-phenylaminopyrimidine [12, 13] and has potent activity against BCR-ABL, the transforming tyrosine kinase found in CML cells [12]. In addition to ABL, imatinib has been reported to inhibit PDGF receptor (PDGFR)-α, PDGFR-β and KIT [14] and FMS [15]. We investigated the effects of imatinib on PDGF mediated proteoglycan size and fine structure and resultant proteoglycan/LDL binding in an *in vitro* cell culture model and further investigated its ability to reduce lipid deposition *ex vivo* and *in vivo* in two mouse models.

Materials and methods

Preparation of human vSMC cultures

Human vSMCs were isolated from otherwise discarded segments of the internal mammary artery from patients undergoing cardiac surgery at the Alfred Hospital (Melbourne, Australia), as previously described [16]. Acquisition and use of tissue conformed to the principles of the Human Ethics Committee of the Alfred Hospital.

Quantitation of radiolabel incorporation into proteoglycans

Quiescent cells were treated in 5 mM glucose DMEM (Invitrogen, Carlsbad, CA, USA), 0.1% FBS, 0.1% DMSO with imatinib (Alfred Hospital Pharmacy, Australia), (0–10 μmol/l) and exposed to Sulfur-35 Na_2SO_4 (1.85 MBq/ml), Tran^{35}S-label (1.85 MBq/ml) or D-glucosamine-HCl, [6–^{3}H] (0.37 MBq/ml), (MP Biomedicals, Solon, OH, USA) under basal conditions or in the presence of PDGF BB (Sigma, St Louis, MO, USA) (50 ng/ml) for 24 hrs. Secreted proteoglycans were harvested and radiolabel incorporation into proteoglycans quantitated using the CPC precipitation assay [17].

Chemical cleavage of glycosaminoglycan chains

Quiescent cells were treated with imatinib (1 μmol/l) in 0.5 ml DMEM, 0.1% FBS under basal conditions and in the presence of PDGF (50 ng/ml) for 12 hrs prior to the addition of Sulfur-35 Na_2SO_4 (1.85 MBq/ml) for a further 16 hrs. Secreted proteoglycans were harvested, isolated and concentrated as described previously [18]. To chemically cleave the GAG chains through a β-elimination reaction, pelleted proteoglycans were treated with sodium borohydride (1 M) in NaOH (50 mmol/l) for 24 hrs at 45°C. The reaction was terminated with glacial acetic acid.

Synthesis of xyloside initiated GAG chains

Quiescent human vSMCs were treated in 0.5 ml DMEM, 0.1% FBS supplemented with methyl β-D-xylopyranoside (xyloside) (0.5 mmol/l) with imatinib (1 μmol/l) under basal conditions and in the presence of PDGF (50 ng/ml) for 4 hrs prior to the addition of Sulfur-35 Na_2SO_4 (1.85 MBq/ml) for a further 24 hrs. Secreted proteoglycans were harvested, isolated and concentrated as described previously [18].

Size analysis of proteoglycan/GAG length by SDS-PAGE and size exclusion chromatography

Proteoglycans, cleaved GAG chains and xyloside associated GAG chains were sized by SDS-PAGE as described previously [17]. Cleaved GAG chains and xyloside associated GAG chains were sized on sepharose CL-6B columns eluted in guanidine buffer as described previously [6]. Data were standardized by calculating K_{av} values which were subsequently converted to molecular weight (MW) values (Daltons) using an equation derived from the study by Wasteson [19] such that $\text{LogMW} = (-2.27\ K_{av}) + 5.45$.

Analysis of disaccharides by fluorophore assisted carbohydrate electrophoresis (FACE)

To analyse the disaccharide composition of GAG chains the FACE method was used as described by Calabro [20]. Human vSMCs were seeded into 75 cm^2 flasks, cultured and rendered quiescent (48 hrs in media containing 0.1% FBS). Cells were treated with imatinib (1 μmol/l) under basal conditions and in the presence of PDGF (50 ng/ml) for 24 hrs. Secreted proteoglycans were harvested and isolated as described above and prepared for FACE as described previously [20] prior to separation on 20% acrylamide gels. Electrophoresis was performed at 500 V, 30 mA per gel for 70 min. at 4°C. Gel images were captured using a FACE imager (Glyko Model SE2000, Hayward, CA, USA, Prozyme, San Leandro, USA) and total pixel densities for individual lanes determined using a public domain image program, ImageJ (National Institutes of Health, Bethesda, MD, USA). Individual monosulphated disaccharide bands were calculated as percentages of the total pixel density of individual lanes.

Analysis of proteoglycan LDL binding by gel mobility shift assay

Human vSMCs were cultured, rendered quiescent as described and treated with imatinib (1 μmol/l) under basal conditions and in the presence of PDGF (50 ng/ml) for 12 hrs at which time fresh treatments were added with Tran^{35}S-label (1.85 MBq/ml) to radiolabel proteoglycan core proteins (37°C, 24 hrs). The secreted proteoglycans were harvested and isolated as described and dialysed into a physiological buffer

(20 mmol/l MOPS, 140 mmol/l NaCl, 5 mmol/l $CaCl_2$, 2 mmol/l $MgCl_2$, pH 7.4). Increasing concentrations of LDL (0–0.5 mg/ml) purified from human blood [21] were incubated with equal counts (1250 cpm) of proteoglycans for 1 hr at 37°C. Samples were run on flat bed agarose gels (0.7%) as described previously [6].

Western blotting

Total cell lysates were resolved on 10% SDS-PAGE and transferred onto PVDF. Membranes were blocked with 5% skim milk powder, incubated with anti-PDGFR-β (Tyr 857) goat monoclonal antibody and followed by HRP-anti-goat IgG and ECL detection (Amersham, Buckinghamshire, UK). Blots from three experiments were quantified by densitometry using ImageJ (NIH) software.

Animal studies

Animal studies were approved by AMREP Animal Ethics Committee and the investigations conformed to the NHMRC (Australia) guidelines. Sixty male homozygous ApoE$^{-/-}$ mice 8 weeks of age (colony at the Baker IDI Heart and Diabetes Institute Precinct Animal Centre, Australia) were maintained in a temperature-controlled facility under a 12-hr light–dark cycle. Mice were given access to food and water *ad libitum*. Mice were fed high fat 'Western' diet (Harlan Teklad TD88137 21% total fat, 0.15% cholesterol) and randomized by weight into four groups ($n = 15$ mice per group) for a 12-week period: Group 1 received a single daily gavage of distilled water (0.1 ml/10 g body weight), Groups 2, 3 and 4 received a single daily gavage of imatinib mesylate dissolved in distilled water at 10, 20 or 40 mg/kg body weight, respectively. Body weights were recorded weekly and baseline plasma cholesterol and triglycerides measured. After 12 weeks mice were fasted overnight and anaesthetized by an intraperitoneal injection of pentobarbitone sodium. Heparinized blood was collected by cardiac puncture to the right ventricle, centrifuged and plasma stored at −20°C for subsequent analysis of total cholesterol and triglycerides. The heart and aorta were excised intact to the iliac bifurcation for assessment of lipid lesion area.

Evaluation of lipid lesion formation

The aorta was used for *en face* evaluation of atherosclerotic lesion area. Aortae were carefully cleaned of adventitia and separated from the heart under a dissecting microscope, split longitudinally and pinned. Lipid deposition in the aorta was visualized as described previously [22]. Sudan IV-positive lesion areas were quantified from digitized images using Optimas image analysis software. All analyses were made in masked fashion by the two investigators. The extent of lipid lesion formation was expressed as the percentage of total aortic surface area.

Measurement of arterial lipid accumulation

Male ApoE$^{-/-}$ mice (10–12 weeks old) received angII (500 ng/kg/min) for 28 days *via* Alzet osmotic minipumps (ALZA Scientific Products, Mountain View, GA, USA) implanted subcutaneously *via* in the scapular region as previously described [23]. Mice were fed mouse chow (Harlan TD2018) with or without added Imatinib (300 mg/kg) *ad libitum* during the angII infusions. To measure arterial lipid accumulation mice were anaesthetized, carotid arteries removed and perfused with fluorescently labelled LDL as described previously [24, 25].

Statistics

Data were analysed for statistical significance using a one-way ANOVA, a multi-factor one-way ANOVA, a two-way ANOVA or a Student's paired t-test as stated. Data are presented as mean ± S.E.M. Results were considered statistically significant at $P < 0.05$ as stated. Normalization of data was performed in some investigations to adjust for control variations between individual experiments.

Results

Imatinib inhibits proteoglycan synthesis and GAG elongation

Imatinib treatment of human vSMC in the presence of PDGF dose dependently decreased ^{35}S-SO_4 incorporation into secreted proteoglycans with a maximal inhibition of 66% at 10 μmol/l imatinib, with an IC_{50} value of approximately 700 nmol/l (Fig. 1A). The imatinib resistant component of proteoglycan synthesis may represent a basal or endogenous component not amenable to pharmacological inhibition. The electrophoretic mobility of complete proteoglycans isolated from human vSMC after treatment with imatinib, was dose dependently increased relative to PDGF treatment alone (Fig. 1B). Under basal conditions imatinib treatment decreased ^{3}H-glucosamine incorporation into GAG chains of secreted proteoglycans by 43%, $P < 0.01$ (Fig. 1C). PDGF stimulated a 77% increase, $P < 0.01$, in ^{3}H-glucosamine incorporation and imatinib treatment decreased this PDGF mediated increase in by 64%, $P < 0.01$ (Fig. 1C). The decrease in radiolabel incorporation from the basal state is most probably due to inhibition of the autocrine action of endogenously produced PDGF [26]. PDGF stimulated proteoglycan core protein synthesis and imatinib treatment decreased ^{35}S-met/cys incorporation by 32%, $P < 0.01$ (Fig. 1D).

SDS-PAGE analysis showed the action of PDGF to decrease the electrophoretic mobility and imatinib treatment to increase mobility of the cleaved GAG chains (Fig. 2A, lane 7 *versus* 8). A representative size exclusion analysis is shown (Fig. 2B). Cleaved GAG chains derived from PDGF treated cells had a mean K_{av} value of 0.45 ± 0.01 compared to control with a mean K_{av} value of 0.47 ± 0.01, $P < 0.05$ (see Table 1). Conversion of K_{av} values to MWs showed an increase in mean GAG chain size with PDGF treatment from 24.2 ± 1.3 kD for control to 26.8 ± 1.4 kD (see Table 1). GAG chains derived after imatinib treatment of human vSMC under basal conditions and in the presence of PDGF showed mean K_{av} values of 0.50 ± 0.02 and 0.49 ± 0.02, $P < 0.05$, respectively, converting to MWs of 20.7 ± 2.2 kD and 21.8 ± 2.3 kD, respectively (see Table 1).

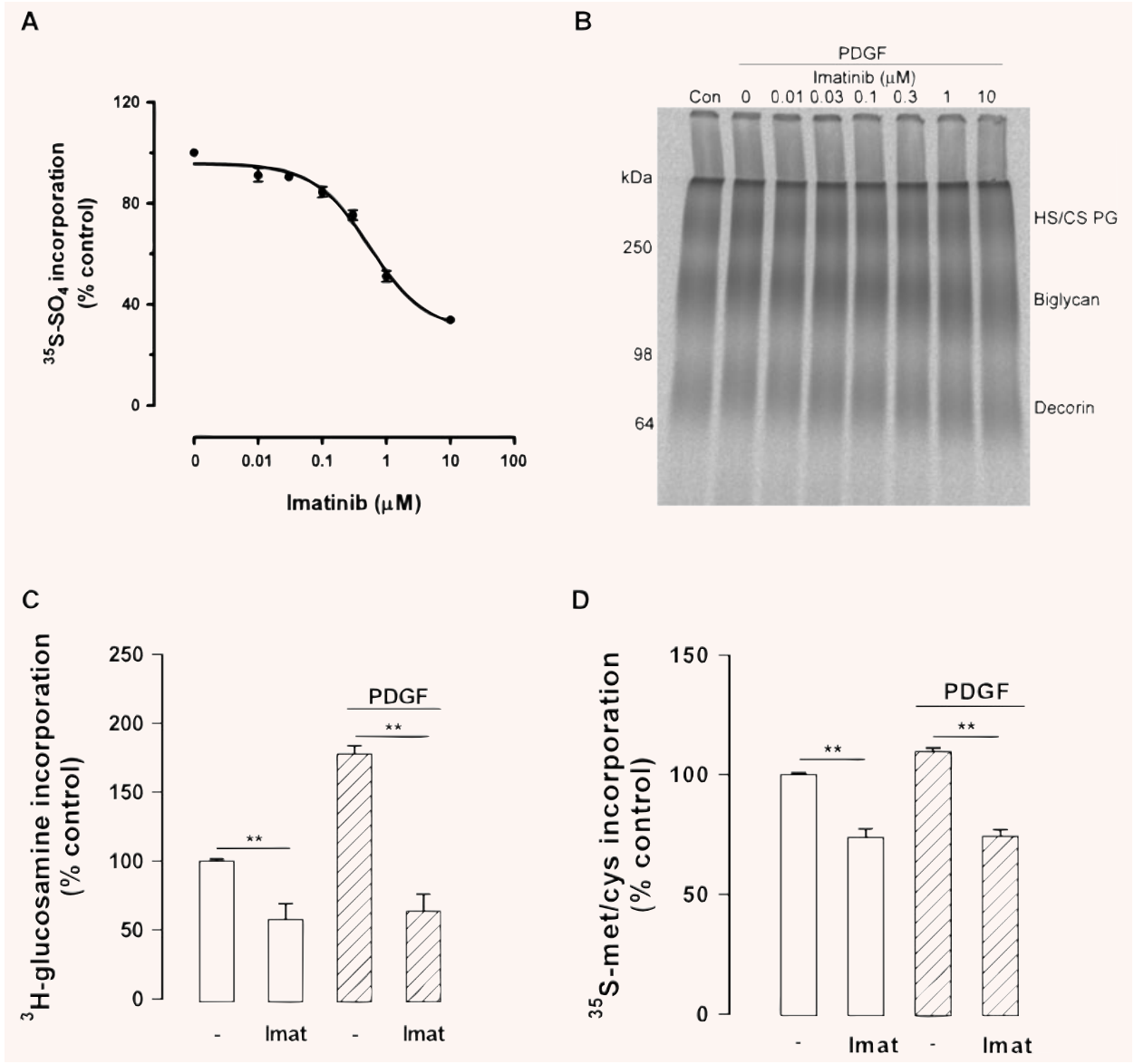

Fig. 1 Imatinib dose dependently decreases radiolabel incorporation into proteoglycans and increases electrophoretic mobility in the presence of PDGF. Human vSMC were treated with imatinib (**A**, **B** 0.01–10 μM, **C**, **D** 1 μM) and PDGF (50 ng/ml) in the presence of (**A**) Sulfur-35 Na_2SO_4 (1.85 MBq/ml) or (**C**) D-glucosamine-HCl, [6–3H] (0.37 MBq/ml) or (**D**) Tran^{35}S-label (1.85 MBq/ml). Media containing secreted proteoglycans was blotted onto chromatography paper and precipitated *via* cetylpyridinium chloride, followed by measurement of radiolabel incorporation. Results are the mean ± S.E.M. of normalized data from three experiments in triplicate, ** $P < 0.01$ using a one-way ANOVA. For the dose–response curve shown in (**A**) IC_{50} value 0.5 μM r^2 0.95. (**B**) Secreted proteoglycans were isolated using ion exchange chromatography (DEAE Sephacel) and concentrated by ethanol precipitation. Proteoglycans were separated on a 4−13% acrylamide gradient gel. Gel was performed twice from two separate experiments, with a representative shown.

Synthesis of GAG chains on a xyloside primer is a technique that allows evaluation of GAG synthesis which is independent of proteoglycan core protein [27]. SDS-PAGE analysis showed identical results to that seen with intact proteoglycans indicating that the action of imatinib on intact proteoglycans was identical to that of xyloside GAGs (Fig. 2A, lanes 1–4; Fig. 2C, lanes 1–4). Treatment of human vSMC with PDGF resulted in xyloside-initiated GAG chains with decreased electrophoretic mobility

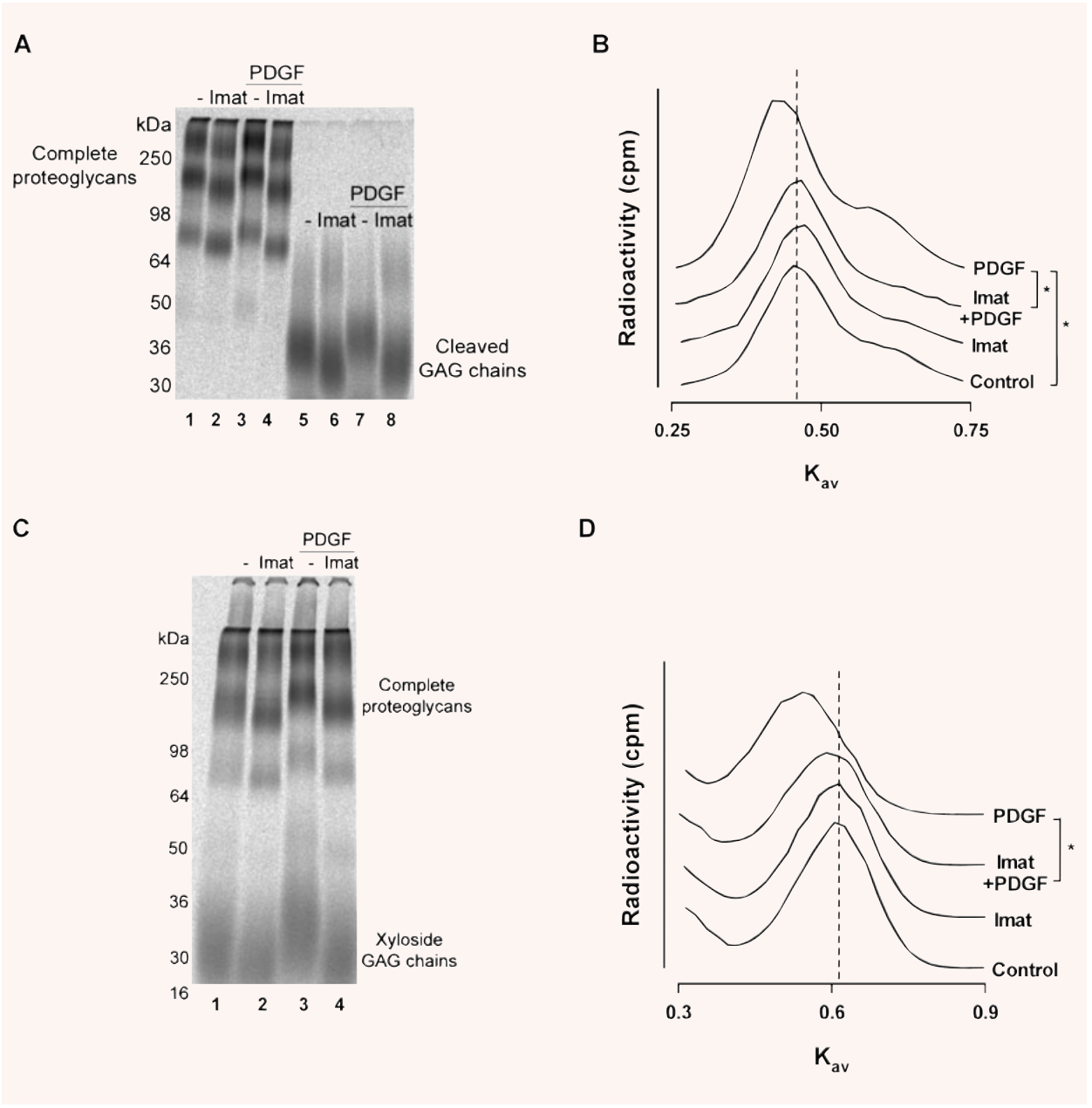

Fig. 2 Imatinib treatment of human vSMCs decreases the size of chemically cleaved and xyloside initiated GAG chains. (**A**) Human vSMC were treated with imatinib (1 μmol/l) and PDGF (50 ng/ml) for 12 hrs then Sulfur-35 Na_2SO_4 (1.85 MBq/ml) was added for a further 16 hrs. Secreted proteoglycans were isolated and concentrated. GAG chains were cleaved from proteoglycan core proteins *via* a β-elimination reaction and were separated by SDS-PAGE on 4–20% acrylamide gradient gels. (**C**) Human vSMC were treated with imatinib (1 μmol/l) and xyloside (0.5 mmol/l) under basal conditions and in the presence of PDGF (50 ng/ml) for 4 hrs prior to the addition of Sulfur-35 Na_2SO_4 (50 μCi/ml) for a further 24 hrs. Secreted proteoglycans and xyloside initiated GAG chains were isolated and concentrated and separated by SDS-PAGE on 4–13% acrylamide gradient gels. In each case gels were performed three times from three separate experiments, with a representative shown. Size analysis of the B cleaved GAG chains and D xyloside associated GAG chains were performed by size exclusion chromatography (sepharose CL-6B). Vertical lines indicate the calculated K_{av} of GAG chains of proteoglycans from control cells. Three measurements were performed from three separate experiments in each case with a representative shown, ** $P < 0.01$ using a paired Student's t-test.

Table 1 Distribution coefficients (K_{av}) and associated MWs for GAG chains using sepharose CL-6B size exclusion chromatography

	Control	Imatinib	PDGF	Imatinib + PDGF
Cleaved chains				
K_{av}	0.47 ± 0.01	0.50 ± 0.02	0.45 ± 0.01*	0.49 ± 0.02#
MW (kD)	24.2 ± 1.3	20.7 ± 2.2	26.8 ± 1.4	21.8 ± 2.3
Xyloside GAGs				
K_{av}	0.60 ± 0.02	0.63 ± 0.02	0.56 ± 0.03	0.62 ± 0.02#
MW (kD)	12.3 ± 1.3	10.5 ± 1.1	15.2 ± 2.4	11.1 ± 1.2

K_{av} values are expressed as the mean ± S.E.M. of three separate size exclusion experiments.
*$P < 0.05$ and #$P < 0.05$ compared to control and PDGF treatment, respectively, using a paired Student's t-test. Calculated MWs are expressed as the mean ± range.

indicating an increase in size (Fig. 2C, lane 1 *versus* 3). Imatinib treatment under basal conditions and in the presence of PDGF caused an increase in the electrophoretic mobility of xyloside GAG chains (Fig. 2C, lanes 2 and 4) indicating inhibition of GAG elongation. PDGF treatment of vSMCs decreased the K_{av} of xyloside initiated GAG chains from 0.60 ± 0.02 for control to 0.56 ± 0.03 (Fig. 2D). Imatinib treatment under basal conditions and in the presence of PDGF increased the K_{av} of the xyloside initiated GAG chains to 0.63 ± 0.02 and 0.62 ± 0.02, respectively (Fig. 2D). PDGF treatment increased xyloside GAG size from 12.3 ± 1.3 kD to 15.2 ± 2.4 kD (see Table 1). Imatinib treatment under basal conditions and in the presence of PDGF decreased xyloside initiated GAG chain size to 10.5 ± 1.1 kD and 11.1 ± 1.2 kD, respectively (see Table 1). Thus imatinib inhibits the biochemical process of GAG elongation which is activated by PDGF.

Imatinib decreases 6:4 position sulphation ratio of disaccharide units

Stimulation of human vSMC with PDGF increased the mean 6:4 position sulphation ratio assessed by FACE from 1.0 to 2.0, $P < 0.01$ (Fig. 3A). This is consistent with previous reports of increases in the 6:4 position sulphation ratio upon stimulation with PDGF [9, 28]. Under basal conditions, imatinib decreased the mean 6:4 sulphation ratio from 1.0 to 0.6, $P < 0.01$ (Fig. 3A). Imatinib treatment in the presence of PDGF decreased the mean 6:4 sulphation ratio from 2.0 to 1.4, $P < 0.01$ (Fig. 3A).

Imatinib decreases proteoglycan/LDL binding

To assess the LDL binding properties of proteoglycans isolated from imatinib treated human vSMC the gel mobility shift assay was used [29]. The half maximal saturation value for control proteoglycans was approximately 0.01 mg/ml LDL compared to 0.04 mg/ml LDL for proteoglycans from imatinib treated cells (Fig. 3B). The half maximal saturation value for proteoglycans from imatinib treated cells in the presence of PDGF was approximately 0.05 mg/ml compared to 0.02 mg/ml for PDGF treatment alone (Fig. 3C), indicating a substantial decrease in LDL binding with imatinib treatment.

Analysis of imatinib actions on vascular lipid deposition in high fat fed ApoE$^{-/-}$ mice

We evaluated the ability of imatinib to reduce lipid deposition *in vivo* in the aortic wall of high fat fed Apo E$^{-/-}$ mice in two models. Firstly by treating ApoE$^{-/-}$ mice with imatinib for 12 weeks and evaluating lipid deposition by *en face* staining of the aorta. At the end of the treatment period there was no significant difference in weight gain between the treated groups of mice including highest dose of imatinib (40 mg/kg) (see Table 2). Even the highest dose of imatinib (40 mg/kg) did not affect body weight. End-point plasma cholesterol of mice in the three imatinib treatment groups were similar cholesterol 27–29 mmol/l and triglyceride 2.5–3.2 mmol/l. Total cholesterol in the 10 and 20 mg/kg treatment groups and triglycerides in the 20 mg/kg group were slightly higher than high-fat diet untreated controls ($P < 0.05$; see Table 2). *En face* staining with Oil red O showed that imatinib significantly reduced the high fat-induced lipid staining area by 30%, 27% and 35% $P < 0.01$ compared to high-fat diet untreated control when dosed by gavage at 10, 20 and 40 mg/kg, respectively (Fig. 4A). The effect of imatinib to inhibit lipid deposition was most effective in the aortic arch region (Fig. 4A). Clearly imatinib reduced lipid deposition even though plasma lipid levels were not reduced.

To determine if decreased LDL retention was the mechanism accounting for the decreased atherosclerosis observed, LDL retention was quantified in carotid arteries from mice that had received angiotensin II (used to increase vascular matrix content [24]) with ($n = 3$) or without ($n = 4$) imatinib in the diet for 28 days. The carotid arteries were alternately perfused with fluorescent LDL or non-fluorescent buffer, thus each artery serves as its own control. Quantitative fluorescence microscopy demonstrated

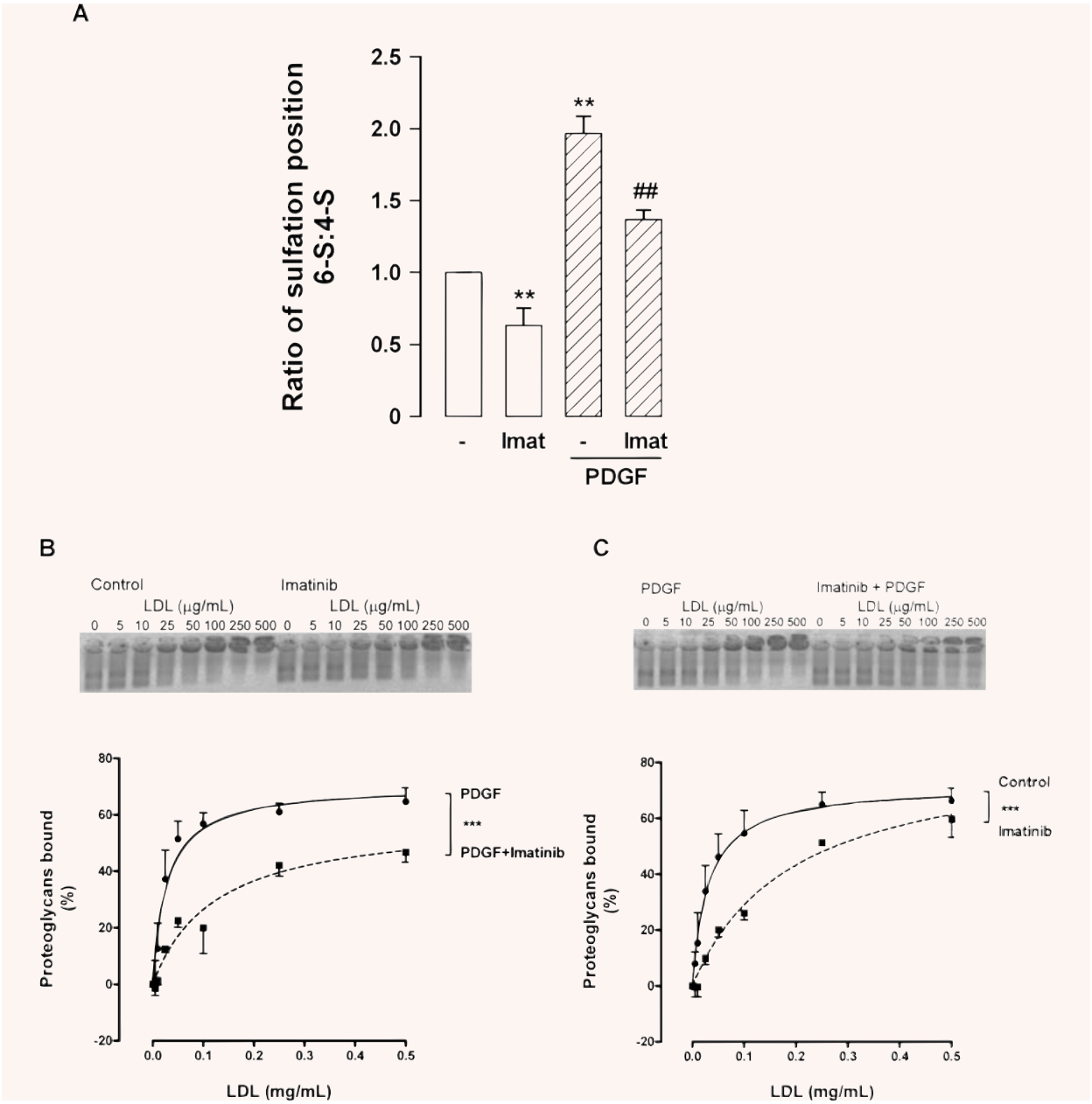

Fig. 3 Imatinib treatment of human vSMC decreases the GAG chain 6:4 position sulphation ratio and results in decreased binding to LDL. (**A**) Human vSMC were treated with imatinib (1 μmol/l) under basal conditions and in the presence of PDGF (50 ng/ml) for 24 hrs. Secreted proteoglycans were isolated, concentrated, dialysed into sterile water and vacuum concentrated. Proteoglycan core proteins were digested (Proteinase K), GAG chains precipitated (ethanol) and digested with chondroitinase (ABC). Disaccharides were then fluorotagged with AMAC and separated (20% acrylamide gel). Images were captured using a FACE imager and the 6:4 position sulphation ratios of monosulphated disaccharides calculated. Normalized data from three separate experiments is shown as mean ± S.E.M., ** $P < 0.01$ *versus* control, ## $P < 0.01$ *versus* PDGF using a one-way ANOVA. Human vSMC were treated with imatinib (1 μmol/l) under B basal conditions and C in the presence of PDGF (50 ng/ml) in the presence of ^{35}S-met/cys (1.85 MBq/ml). Core protein radiolabelled proteoglycans were isolated and equal counts combined with increasing concentrations of LDL. Flat bed agarose gels were utilized for separation and calculation of bound and free proteoglycans was performed with image analysis software. Three separate experiments were performed, with a representative gel shown and results shown as mean ± S.E.M., *** $P < 0.001$ using a two-way interaction ANOVA comparing the two data sets. Half maximal saturation binding values: Control 0.031 mg/ml, Imatinib 0.193 mg/ml, PDGF 0.028 mg/ml, PDGF + Imatinib 0.123 mg/ml.

Table 2 Metabolic parameters of mice at the end of treatment

	Control	Imatinib 10 mg/kg	Imatinib 20 mg/kg	Imatinib 40 mg/kg
Body weight gain (g)	9.3 ± 0.4	8.9 ± 0.5	9.3 ± 0.5	9.9 ± 0.5
Total cholesterol (mmol/l)	23.1 ± 1.2	27.4 ± 1.3*	29.2 ± 1.6*	27.2 ± 1.8
Triglycerides (mmol/l)	2.4 ± 0.3	3.2 ± 0.2	3.3 ± 0.2*	2.5 ± 0.4
LDL (mmol/l)	17.7 ± 1.0	20.9 ± 1.0	22.2 ± 1.2	21.0 ± 1.4
HDL (mmol/l)	4.4 ± 0.3	5.0 ± 0.2	5.5 ± 0.3	5.1 ± 0.3
Ratio LDL/HDL	4.2 ± 0.2	4.1 ± 0.1	4.0 ± 0.1	4.0 ± 0.1

Data are expressed as mean ± S.E.M., $n = 13$–15 per group.

*$P < 0.05$ compared to high-fat diet untreated control using a paired Student's t-test.

a trend towards decreased LDL retention in mice that received imatinib (13.5 ± 2.5 *versus* 9.2 ± 1.1 arbitrary units for control *versus* imatinib, respectively, P = 0.2).

Effect of imatinib on the PDGF receptor phosphorylation in human vascular smooth muscle cells

We examined PDGFR phosphorylation following exposure of human vSMCs to PDGF. We performed Western blot analysis of the growth factor PDGF-mediated phosphorylation of the autophosphorylation activation site of the PDGFR (Tyr 857). PDGF markedly increased phosphotyrosine 857 levels on PDGFR reaching a peak around 30 min. (data not shown). To investigate the action of imatinib on PDGFR signalling we treated cells with imatinib (1 μmol/l) in the absence and presence of PDGF (50 ng/ml, 20 min.) and demonstrated that imatinib almost completely abolished the PDGF-mediated phosphorylation of tyrosine 857 of PDGFR (Fig. 4B).

Discussion

Proteoglycans play a crucial role in the binding and retention of LDL in early human atherosclerosis [3, 4]. Imatinib inhibited GAG synthesis and reduced LDL binding to proteoglycans *in vitro* and reduced aortic lipid deposition in a high fat fed mouse model *in vivo*. This is in agreement with the Lassila *et al.* study that observed decreased plaque area in a diabetic ApoE knockout mouse model of atherosclerosis but which they attributed to inhibition of vSMC proliferation [30]. Imatinib treatment blocked the autophosphorylation of Tyr857 of the PDGFRβ. Imatinib treatment of human vSMC blocked the PDGF action to elongate GAG chains on vascular proteoglycans. Imatinib treatment also decreased the 6:4 position sulphation ratio of monosulphated disaccharides. Both these latter actions have implications for binding of LDL by proteoglycans. The extent of LDL binding to proteoglycans derived after imatinib treatment revealed a substantial decrease in LDL binding under basal conditions and in the presence of PDGF. GAG chain length is a key determinant of LDL binding [18, 31]. Angiotensin II increases the size of proteoglycans that bind LDL with 2.5- to 3-fold higher affinity than controls [32]. Oxidized LDL stimulates the synthesis and increases GAG chain size on versican, biglycan and decorin which have a high affinity for LDL [33]. Vascular SMCs grown on extracellular matrix synthesize larger proteoglycans with a high affinity for LDL binding [31]. Conversely, a decrease in GAG chain size is associated with decreased binding to LDL [6, 34]. Proteoglycans synthesized in the presence of troglitazone and their chemically cleaved chains are smaller and bind LDL with a lower affinity [34]. Proteoglycans and xyloside initiated GAG chains synthesized in the presence of glucosamine exhibit a decrease in size and a lower LDL binding [18]. Proteoglycans synthesized in the presence of fenofibrate [6] and amlodipine [35] are decreased in size and have a decreased LDL binding. The decrease in GAG chain size with imatinib treatment has most likely contributed greatly to the decrease in LDL binding detected in this study.

The effect of imatinib to decrease the 6:4 position sulphation ratio may also impact on LDL binding although this is less clear. Sulphation at the exocyclic 6 position is more likely to be sterically accessible to LDL particles compared to sulphation at the 4 position. In agreement with this notion is the finding that the atherosclerosis-susceptible White Carneau pigeon has an increase in 6 position sulphation compared to the atherosclerosis-resistant Show Racer pigeon [36]. Furthermore, stimulation of non-human primate aortic SMC with the atherogenic growth factor PDGF increases the 6:4 position sulphation ratio [9]. The possible mechanism by which imatinib decreases 6 position sulphation may be inhibition of the activity or expression of a specific 6-sulfotransferase(s).

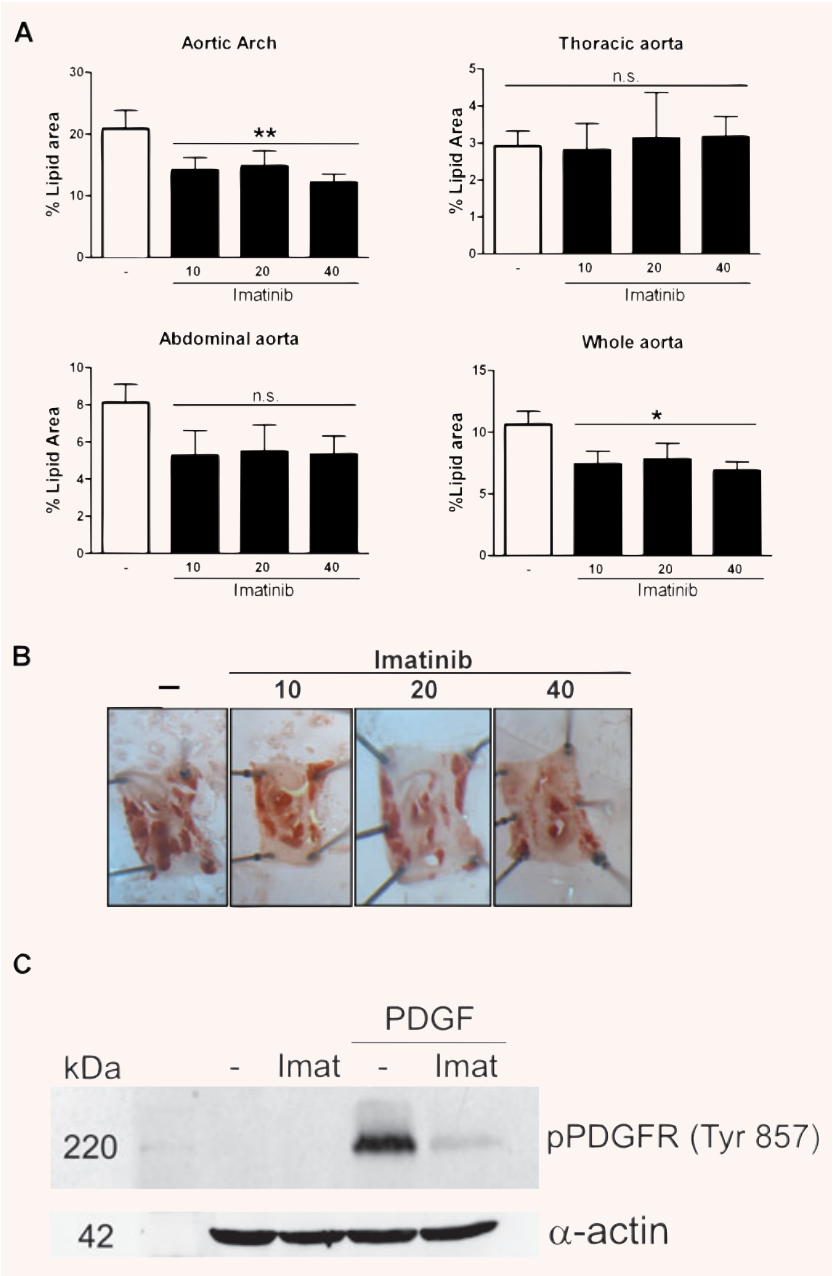

Fig. 4 Imatinib decreases lipid area in ApoE$^{-/-}$ mice and blocks PDGFR autophosphorylation. (**A**) Eight-week-old ApoE$^{-/-}$ mice ($n = 15$ per group) were fed a high fat diet and treated for 12 weeks with imatinib (at 10, 20 or 40 mg/kg body weight, respectively) by daily gavage. The proportion of aortic surface area stained with Sudan-IV for lipid was analysed *en face* by image analysis. Results are shown as mean ± S.E.M., * $P < 0.05$ using a multi-factor one-way ANOVA. (**B**) Representative examples of aortic arch of ApoE$^{-/-}$ mice fed a high fat diet and treated for 12 weeks with imatinib (at 10, 20 or 40 mg/kg body weight, respectively) by daily gavage. Aortic surface was stained with Sudan-IV to identify lipid-rich plaques. (**C**) Effect of imatinib on tyrosine phosphorylation on the autophosphorylation site (Tyr857) of the PDGF receptor. Western blot of human vSMC from imatinib-treated cells (Imat lanes 3 and 5) in the absence (lane 3) or presence of PDGF (50 ng/ml) for 20 min. (lane 5). Samples were lysed and subjected to 10% SDS-PAGE. Phospho-PDGFR-β was visualized using anti-phosphotyrosine 857 antibody and anti-goat-HRP conjugated antibody followed by ECL detection. Membranes were reprobed with anti-smooth muscle α-actin and antimouse-HRP conjugated antibody.

Having established that imatinib inhibits GAG synthesis and reduces LDL binding *in vitro*, the consequences of imatinib treatment on vascular lipid deposition in an animal model were assessed. Treatment of high-fat fed ApoE knockout mice with imatinib appreciably reduced the area of lipid deposition in the aorta, particularly in the aortic arch region. The modest reduction in lipid deposition may reflect the different initiation, location and progression of atherosclerosis in mouse models compared to the early stages of human atherosclerosis [37, 38]. Initiation and progression of the disease in mice is macrophage-rich however in human beings it is a smooth muscle cell rich environment with extracellular matrix rich in proteoglycans. A question from this work is if there are imatinib-induced changes in GAG length in the vessel wall. We attempted to experimentally assess GAG elongation in the aorta wall *in vivo*. Proteoglycans were isolated from mouse aorta and GAG chains cleaved and radiolabelled using

tritiated sodium borohydride. At this stage it appears that this technique does not have the sensitivity to pick up the changes in GAG length that may be occurring in a population of CS/DS proteoglycans. There are no other viable techniques available, such as the measurement of the expression of a CS GAG polymerization enzyme [8] to demonstrate GAG chain length in vessel walls. We continue to work on this important question.

Our results support previous studies [30, 39] which report anti-atherogenic roles for imatinib. In low-density lipoprotein receptor knockout ($LDLR^{-}$)/$SM22Cre^{+}$; $LRP^{flox/flox}$ knockout ($smLRP^{-}$) mice, imatinib treatment reduced total atherosclerotic lesion area by approximately 50% [39]. In that study, Boucher *et al.* investigated the role of LDLR related protein (LRP) in modulating PDGF signalling to protect against atherosclerosis by decreasing migration and proliferation of cells. Hyperactivity of the PDGF pathway was noted in $LDLR^{-}$ /$smLRP^{-}$ mice and this could have resulted in stimulation of GAG elongation on vascular proteoglycans leading eventually to increased formation of atherosclerotic plaques. Although the decrease in atherosclerotic lesion development after imatinib treatment in this animal model was ascribed to inhibition of migration and proliferation *via* inhibition of the PDGFR by imatinib, it is also feasible that imatinib acted to inhibit PDGF stimulated GAG elongation on vascular proteoglycans, reduced lipid binding and thereby contributed to a decrease in total atherosclerotic lesion area. In mouse models of atherosclerosis, including our model using $ApoE^{-\backslash-}$ mice, biglycan and perlecan but not versican are the key proteoglycans observed in lesions [40]. PDGF does not stimulate biglycan mRNA in vSMC *in vitro* [9] or perlecan mRNA, indeed it reduces perlecan mRNA levels. Thus the effect of imatinib to reduce lipid binding is unlikely to be mediated *via* an increase in these proteoglycan mRNA levels. In addition it is not known to what extent proteoglycans produced by cells other than vSMCs contribute to lipid deposition in this model.

Imatinib is a protein tyrosine kinase inhibitor which inhibits PDGFR-α and -β, KIT, ABL and FMS [15]. We demonstrate that imatinib inhibits PDGFR tyrosine 857 phosphorylation, the first step in a cascade of intracellular signalling that affects GAG elongation in vSMCs. The actions of imatinib to inhibit PDGF stimulation of GAG elongation, decrease binding of vascular proteoglycans to LDL and reduce the deposition of lipid in the vessel wall may potentially lead to a reduction in the development or progression of atherosclerosis. The prevention of GAG elongation may represent a therapeutic target for the prevention of atherosclerosis and such investigations are currently underway in our laboratory

There is currently an epidemic of obesity leading to insulin resistance, pancreatic β cell destruction and type 2 diabetes, the latter of which is a major risk factor for cardiovascular disease. This phenomenon has the potential to generate sufficient morbidity to overwhelm health systems. Our data show that imatinib modifies the synthesis and structure of proteoglycan leading to reduced binding to LDL and reduced deposition of lipid in the vessel wall. Independently, imatinib inhibits the development of insulin resistance and also offers β cell protection [41], both actions associated with prevention of type 1 and type 2 diabetes [42]. Thus, imatinib has the potential to limit the development of diabetes-associated atherosclerosis making this therapeutic strategy worthy of further investigation for addressing the epidemic of diabetes-driven cardiovascular disease.

Acknowledgements

This work was supported by a National Health and Medical Research Council Project Grant ID 268928, Diabetes Australia Research Trust Grant and National Heart Foundation Grant (to P.J.L.), by National Institutes of Health Grant HL082772 (to L.R.T.) and HL055667 (to J.C.R.). M.L.B. was supported by an Australian Post-Graduate Award from the Department of Education, Science and Training. We thank Kylie Gilbert, Nada Stefanovic and Phyllis Chew for their excellent work, assistance and dedication to the project.

References

1. **Hozawa A, Folsom AR, Sharrett AR, *et al.*** Absolute and attributable risks of cardiovascular disease incidence in relation to optimal and borderline risk factors: comparison of African American with white subjects – Atherosclerosis Risk in Communities Study. *Arch Intern Med.* 2007; 167: 573–9.
2. **Ross R.** The pathogenesis of atherosclerosis: a perspective for the 1990s. *Nature.* 1993; 362: 801–9.
3. **Nakashima Y, Fujii H, Sumiyoshi S, *et al.*** Early human atherosclerosis: accumulation of lipid and proteoglycans in intimal thickenings followed by macrophage infiltration. *Arterioscler Thromb Vasc Biol.* 2007; 27: 1159–65.
4. **Torzewski M, Navarro B, Cheng F, *et al.*** Investigation of Sudan IV staining areas in aortas of infants and children: possible prelesional stages of atherogenesis. *Atherosclerosis* 2009; 206: 59–167.
5. **Williams KJ, Tabas I.** The response-to-retention hypothesis of early atherogenesis. *Arterioscler Thromb Vasc Biol.* 1995; 15: 551–61.
6. **Ballinger ML, Nigro J, Frontanilla KV, *et al.*** Regulation of glycosaminoglycan structure and atherogenesis. *Cell Mol Life Sci.* 2004; 61: 1296–306.
7. **Little PJ, Ballinger ML, Osman N.** Vascular wall proteoglycan synthesis and structure as a target for the prevention of atherosclerosis. *Vascular Health Risk Management.* 2007; 3: 1–8.
8. **Little PJ, Ballinger ML, Burch ML, *et al.*** Biosynthesis of natural and hyperelongated chondroitin sulfate glycosaminoglycans: new insights into an elusive process. *Open Biochem J.* 2008; 2: 135–42.
9. **Schonherr E, Jarvelainen HT, Kinsella MG, *et al.*** Platelet-derived growth factor and transforming growth factor-beta 1 differentially affect the synthesis of biglycan and decorin by monkey arterial smooth

muscle cells. *Arterioscler Thromb.* 1993; 13: 1026–36.

10. **Schonherr E, Kinsella MG, Wight TN.** Genistein selectively inhibits platelet-derived growth factor- stimulated versican biosynthesis in monkey arterial smooth muscle cells. *Arch Biochem Biophys.* 1997; 339: 353–61.
11. **Schindler T, Bornmann W, Pellicena P, *et al.*** Structural mechanism for STI-571 inhibition of abelson tyrosine kinase. *Science.* 2000; 289: 1938–42.
12. **Druker BJ, Tamura S, Buchdunger E, *et al.*** Effects of a selective inhibitor of the Abl tyrosine kinase on the growth of Bcr-Abl positive cells. *Nat Med.* 1996; 2: 561–6.
13. **Buchdunger E, Zimmermann J, Mett H, *et al.*** Inhibition of the Abl protein-tyrosine kinase in vitro and in vivo by a 2-phenylaminopyrimidine derivative. *Cancer Res.* 1996; 56: 100–4.
14. **Buchdunger E, Cioffi CL, Law N, *et al.*** Abl protein-tyrosine kinase inhibitor STI571 inhibits in vitro signal transduction mediated by c-kit and platelet-derived growth factor receptors. *J Pharmacol Exp Ther.* 2000; 295: 139–45.
15. **Dewar AL, Cambareri AC, Zannettino AC, *et al.*** Macrophage colony-stimulating factor receptor c-fms is a novel target of imatinib. *Blood.* 2005; 105: 3127–32.
16. **Neylon CB, Little PJ, Cragoe EJ Jr, *et al.*** Intracellular pH in human arterial smooth muscle. Regulation by Na+/H+ exchange and a novel 5-(N-ethyl-N-isopropyl) amiloride-sensitive Na(+)- and HCO3(-)-dependent mechanism. *Circ Res.* 1990; 67: 814–25.
17. **Nigro J, Dilley RJ, Little PJ.** Differential effects of gemfibrozil on migration, proliferation and proteoglycan production in human vascular smooth muscle cells. *Atherosclerosis.* 2002; 162: 119–29.
18. **Kawakami S, Arai G, Hayashi T, *et al.*** PPARgamma ligands suppress proliferation of human urothelial basal cells *in vitro*. *J Cell Physiol.* 2002; 191: 310–9.
19. **Wasteson A.** A method for the determination of the molecular weight and molecular-weight distribution of chondroitin sulphate. *J Chromatogr.* 1971; 59: 87–97.
20. **Calabro A, Benavides M, Tammi M, *et al.*** Microanalysis of enzyme digests of hyaluronan and chondroitin/dermatan sulfate by fluorophore-assisted carbohydrate electrophoresis (FACE). *Glycobiology.* 2000; 10: 273–81.
21. **Heinecke JW, Baker L, Rosen H, *et al.*** Superoxide-mediated modification of low density lipoprotein by arterial smooth muscle cells. *J Clin Invest.* 1986; 77: 757–61.
22. **Chew P, Yuen DY, Koh P, *et al.*** Site-specific antiatherogenic effect of the antioxidant ebselen in the diabetic apolipoprotein E-deficient mouse. *Arterioscler Thromb Vasc Biol.* 2009; 29: 823–30.
23. **Daugherty A, Manning MW, Cassis LA.** Angiotensin II promotes atherosclerotic lesions and aneurysms in apolipoprotein E-deficient mice. *J Clin Invest.* 2000; 105: 1605–12.
24. **Huang F, Thompson JC, Wilson PG, *et al.*** Angiotensin II increases vascular proteoglycan content preceding and contributing to atherosclerosis development. *J Lipid Res.* 2008; 49: 521–30.
25. **Walsh BA, Mullick AE, Walzem RL, *et al.*** 17beta-estradiol reduces tumor necrosis factor-alpha-mediated LDL accumulation in the artery wall. *J Lipid Res.* 1999; 40: 387–96.
26. **Libby P, Warner SJ, Salomon RN, *et al.*** Production of platelet-derived growth factor-like mitogen by smooth-muscle cells from human atheroma. *N Engl J Med.* 1988; 318: 1493–8.
27. **Fritz TA, Esko JD.** Xyloside Priming of Glycosaminoglycan Biosynthesis and Inhibition of Proteoglycan Assembly. In: Iozzo RV, editor. Proteoglycan protocols. Totowa, NJ: Humana Press, Inc.; 2001. pp. 317–24.
28. **Schonherr E, Jarvelainen HT, Sandell LJ, *et al.*** Effects of platelet-derived growth factor and transforming growth factor-beta 1 on the synthesis of a large versican-like chondroitin sulfate proteoglycan by arterial smooth muscle cells. *J Biol Chem.* 1991; 266: 17640–7.
29. **Hurt-Camejo E, Camejo G, Sartipy P.** Measurements of proteoglycan-lipoprotein interaction by gel mobility shift assay. *Methods Mol Biol.* 1998; 110: 267–79.
30. **Lassila M, Allen TJ, Cao Z, *et al.*** Imatinib attenuates diabetes-associated atherosclerosis. *Arterioscler Thromb Vasc Biol.* 2004; 24: 935–42.
31. **Vijayagopal P, Menon PV.** Varied low density lipoprotein binding property of proteoglycans synthesized by vascular smooth muscle cells cultured on extracellular matrix. *Atherosclerosis.* 2005; 178: 75–82.
32. **Figueroa JE, Vijayagopal P.** Angiotensin II stimulates synthesis of vascular smooth muscle cell proteoglycans with enhanced low density lipoprotein binding properties. *Atherosclerosis.* 2002; 162: 261–8.
33. **Chang MY, Potter-Perigo S, Tsoi C, *et al.*** Oxidized low density lipoproteins regulate synthesis of monkey aortic smooth muscle cell proteoglycans that have enhanced native low density lipoprotein binding properties. *J Biol Chem.* 2000; 275: 4766–73.
34. **Tannock LR, Little PJ, Tsoi C, *et al.*** Thiazolidinediones reduce the LDL binding affinity of non-human primate vascular cell proteoglycans. *Diabetologia.* 2004; 47: 837–43.
35. **Vijayagopal P, Subramaniam P.** Effect of calcium channel blockers on proteoglycan synthesis by vascular smooth muscle cells and low density lipoprotein-proteoglycan interaction. *Atherosclerosis.* 2001; 157: 353–60.
36. **Edwards IJ, Wagner WD.** Distinct synthetic and structural characteristics of proteoglycans produced by cultured artery smooth muscle cells of atherosclerosis-susceptible pigeons. *J Biol Chem.* 1988; 263: 9612–20.
37. **Rader DJ, Daugherty A.** Translating molecular discoveries into new therapies for atherosclerosis. *Nature.* 2008; 451: 904–13.
38. **Finn AV, Kramer MC, Vorpahl M, *et al.*** Pharmacotherapy of coronary atherosclerosis. *Expert Opin Pharmacother.* 2009; 10: 1587–603.
39. **Boucher P, Gotthardt M.** LRP and PDGF signaling: a pathway to atherosclerosis. *Trends Cardiovasc Med.* 2004; 14: 55–60.
40. **Kunjathoor VV, Chiu DS, O'Brien KD, *et al.*** Accumulation of biglycan and perlecan, but not versican, in lesions of murine models of atherosclerosis. *Arterioscler Thromb Vasc Biol.* 2002; 22: 462–8.
41. **Han MS, Chung KW, Cheon HG, *et al.*** Imatinib mesylate reduces endoplasmic reticulum stress and induces remission of diabetes in db/db mice. *Diabetes.* 2009; 58: 329–36.
42. **Little PJ, Cohan N, Morahan GM.** Potential of small molecule tyrosine kinase inhibitors as immuno-modulators and inhibitors of the development of diabetes. *ScientificWorldJournal.* 2009; 9: 224–8.